

PRODUCT USER MANUAL

FIRE RADIATIVE POWER

PRODUCTS: FRP_PIXEL (LSA-502), FRP_Grid (LSA-503)



Reference Number:
Issue/Revision Index:
Last Change:

SAF/LAND/KCL/PUM_FRP/2.2
Issue 1
19/02/2016

DOCUMENT SIGNATURE TABLE

	Name	Date	Signature
Prepared by :	Martin Wooster, Jiangping He, Weidong Xu, Alessio Lattanzio.		
Approved by :			

DOCUMENTATION CHANGE RECORD

Doc Revision	Issue /	Date	Product Release	Description :
Version 1.0			0.82	Preliminary version
Version 1.1			0.90	After RIDs ORR3 : FRP PIXEL VB0.82
Version 1.2			1.1	Modifications for the ORR3 close-out: FRP_PIXEL V1.1 <ul style="list-style-type: none"> Section 4.4 added Added location of the ancillary file in the LSASAF web page Added explanation on the separation of the output in two files Added explanations on the FRP pixel retrieval Added more information on the different fields of the FRP_PIXEL list product Changed Quality flag coding array
Version 1.3			1.3	Modifications based on the ORR3 close-out: FRP_PIXEL v1.3 <ul style="list-style-type: none"> Clarified description of certain of the fields of the FRP_PIXEL list product and added fields related to each separate uncertainty component Section 4.2 made more explicit with regard to situations where FRP cannot be estimated from a detected fire pixel Ensured target accuracy listed in the PUM is the same as that from the Validation Report Highlighted that FRP_GRID product is produced at present purely for test purposes
Version 1.4			1.4	Updates made to the FRP_Grid descriptions

Version 2.0		2.0	<p>Including the modifications for porting the FRP c code into Python:</p> <ul style="list-style-type: none"> • Clarify the description of SAF NWC cloud mask modification; • Atmosphere correction coefficient from MODTRAN; • Take off cloud edge test.
Version 2.2		1	Reference new papers in ACP describing the product.

Table of Contents

1	Introduction	9
2	FRP Product Purpose	14
3	Product and Algorithm description	15
3.1	FRP-PIXEL Product	16
3.1.1	Inputs	18
3.1.2	Outputs	19
3.2	FRP-GRID Product	19
3.2.1	Inputs	23
3.2.2	Outputs	23
4	Output Data Description.....	23
4.1	Overview.....	23
4.2	FRP_PIXEL	24
4.2.1	Fire list product file.....	25
4.2.2	The FRP-PIXEL Quality Product file	28
4.3	FRP-GRID.....	30
4.4	FRP-PIXEL Product Accuracy and Product Uncertainty	33
4.5	Summary of Product Characteristics.....	35
5	References	37
6	Developers	39

Appendices

List of Figures

Figure 1. The seven-year (2008-2013) per-pixel mean FRP across the SEVIRI disk	11
Figure 2. Spatial variation of SEVIRI nominal pixel area	12
Figure 3. Flowchart showing the FRP-PIXEL processing steps	18
Figure 4. Example of LSA SAF FRP-GRID product content	21
Figure 5. Flowchart showing the FRP-GRID processing steps	22
Figure 6. Example of an FRP-PIXEL List Product file structure	27
Figure 7. Example of FRP-PIXEL Quality Product (13:00 UTC on 5 th July 2015)	30

List of Tables

Table 1 LSA SAF products operational or under-development at the beginning of the 3 rd phase of the project.	14
Table 2 FRP-PIXEL processing steps	19
Table 3 FRP-GRID processing steps	20
Table 4 Parameters used to define spatio-temporal resoln of FRP-GRID product	23
Table 5 FRP-PIXEL datasets stored in list format (one value for each fire pixel)	26
Table 6 FRP-PIXEL datasets stored as 2D matrix in Quality Product (every pixel)	29
Table 7 Coding flags used within the FRP-PIXEL Quality Product files	30
Table 8 FRP-GRID datasets stored as 2D matrix	31
Table 9: Compressed and uncompressed size of the two FRP-PIXEL output files	36

List of Acronyms

APL:	Algorithm Private Layer
ASCAT:	Advanced Scatterometer
ATBD:	Algorithm Theoretical Basis Document
AVHRR:	Advanced Very High Resolution Radiometer
BT:	Brightness Temperature
BTD:	Brightness Temperature Difference
ECMWF:	European Centre for Medium-Range Weather Forecasts
EPS:	EUMETSAT Polar System
EUMETSAT:	European Meteorological Satellite Organisation
FRE:	Fire Radiative Energy
FRP:	Fire Radiative Power
HDF	Hierarchical Data Format
IPMA:	Instituto Português do Mare da Atmosfera
IR:	Infrared Radiation
KCL	King's College London
LUT:	Look-Up Table
METEOSAT:	Geostationary Meteorological Satellite
MIR	Mid-Infrared
MSG:	Meteosat Second Generation
MW:	Megawatts
NASA:	National Air and Space Administration
NIR	Near Infrared Radiation
NWC:	NoWCasting SAF
NWP:	Numerical Weather Prediction
PCL:	Product Command Layer
PDL:	Product Data Layer
ROI:	Region of Interest
SAF:	Satellite Application Facility
SEVIRI:	Spinning Enhanced Visible and InfraRed Imager
TCWV:	Total Column Water Vapour
TIR:	Thermal Infrared
U-MARF:	Unified Meteorological Archiving and Retrieval Facility
VIS:	Visible Radiation

Reference Documents

[RD 1] EUMETSAT (2008). SAF for Land Surface Analysis: Validation Report FRP. SAF for Land Surface Analysis, Report SAF/LAND/IM/VR FRP/I 08, 114p.

[RD 2] EUMETSAT (2009). Fire Radiative Power Product User Manual. Technical Report SAF/LAND/IM/PUM FRP/1.1, EUMETSAT.

[RD 3] EUMETSAT (2015). SAF for Land Surface Analysis: Validation Report FRP. SAF for Land Surface Analysis, Report SAF/LAND/IM/VR FRP/II 10, 40p.

[RD 4] Govaerts, Y.M. Wooster M. Lattanzio A., Roberts G. (2009) MSG SEVIRI Fire Radiative Power (FRP) characterization Algorithm Theoretical Basis Document Version 2.2, Report No EUM/MET/SPE/06/0398, 2009

[RD 5] Govaerts, Y.M. Wooster, Roberts, G., Freeborn, P., XU, W., He, J. and Lattanzio A (2015) MSG SEVIRI Fire Radiative Power (FRP) characterization Algorithm Theoretical Basis Document Version 2.8, Report No EUM/MET/SPE/06/0398, 2015

1 Introduction

This product user manual (PUM) relates to the fire radiative power (FRP) products generated at the Satellite Application Facility (SAF) on Land Surface Analysis (LSA). These products target the detection and characterisation of landscape scale fires burning on the Earth surface, and two FRP products namely the FRP-PIXEL (LSA-502) and FRP-GRID (LSA-503) products are derived using data from SEVIRI, which operates on-board the Meteosat Second Generation (MSG) series of geostationary EO satellites. Readers are referred to the papers Wooster *et al.* (2015) and Roberts *et al.* (2015), along with their respective supplements, that appeared in the peer-reviewed Journal *Atmospheric Chemistry and Physics*, as a further source of information on these products.

The LSA SAF is part of the SAF Network, a set of specialised development and processing centres, serving as a EUMETSAT (European organization for the Exploitation of Meteorological Satellites) distributed Applications Ground Segment. The SAF network complements the product-oriented activities at the EUMETSAT Central Facility in Darmstadt, and its primary purpose is to take full advantage of remotely sensed data, particularly those available from EUMETSAT sensors, to measure land surface variables, which will find primarily applications in meteorology (<http://lsa-saf.eumetsat.int/>). The LSA SAF is headquartered at IMPA (Lisbon), and the LSA SAF partner with responsibility for development and maintenance of the FRP products is King's College London (<http://wildfire.geog.kcl.ac.uk/>).

Currently the LSA SAF FRP products are generated from observations made by the Meteosat geostationary satellite. The spin-stabilised Meteosat Second Generation (MSG) satellite has an imaging-repeat cycle of 15 minutes. The Spinning Enhanced Visible and Infrared Imager (SEVIRI) radiometer embarked on the MSG platform encompasses unique spectral characteristics and accuracy, with a 3 km pixel sampling distance at nadir (1 km for the high-resolution visible channel), and 12 spectral channels (Schmetz *et al.*, 2002). FRP products are generated at the full spatio-temporal resolution of the level 1b SEVIRI data, as well as at a lower spatio-temporal resolution where certain bias correction adjustments are made.

Products from the EUMETSAT Polar System (EPS) are also generated at the LSA SAF, though not FRP products currently as the AVHRR imager carried by EPS has its 3.7 micron channel observations (which are necessary for the FRP application) replaced by 1.6 micron channel observations by day when fires are most active. Many other LSA SAF products are, however, generated from EPS data, and EPS is Europe's first polar orbiting operational meteorological satellite, as well as being the European contribution to a joint polar system with the U.S. EUMETSAT will have the operational responsibility for the "morning orbit" with Meteorological-Operational (MetOp) satellites, the first of which was successfully launched on October 19, 2006. Despite the wide range of sensors on-board MetOp (<http://www.eumetsat.int>), in terms of the LSA SAF most of the generated data products make use of the Advanced Very

High Resolution Radiometer (AVHRR) and, to a lesser extent, the Advanced Scatterometer (ASCAT).

Several studies have stressed the role of land surface processes on weather forecasting and climate modelling (e.g., Dickinson *et al.*, 1983; Mitchell *et al.*, 2004; Ferranti and Viterbo, 2006). The LSA SAF has been especially designed to serve the needs of the meteorological community, particularly Numerical Weather Prediction (NWP). However, there is no doubt that the LSA SAF addresses a much broader community, which includes users from:

- Weather forecasting and climate modelling, requiring detailed information on the nature and properties of land.
- Environmental management and land use, needing information on land cover type and land cover changes (e.g. provided by biophysical parameters or thermal characteristics).
- Agricultural and Forestry applications, requiring information on incoming/outgoing radiation and vegetation properties.
- Renewable energy resources assessment, particularly biomass, depending on biophysical parameters, and solar energy.
- Natural hazards management, requiring frequent observations of terrestrial surfaces in both the solar and thermal bands.
- Climatological applications and climate change detection, requiring long and homogeneous time-series.
- Chemical weather and air quality, requiring information on fire detection and intensity.

The LSA SAF products (Table 1) are based on either level 1.5 SEVIRI/Meteosat and/or level 1b MetOp datasets. Forecasts provided by the European Centre for Medium-range Weather Forecasts (ECMWF) are also used as ancillary data, most usually for atmospheric correction of the top-of-atmosphere spectral radiances.

The Meteosat derived LSA SAF products are now derived and provided as full Earth disk products. Access to these may be requested at the LSA SAF website (<http://landsaf.ipma.pt>), and are also distributed in near real time via FTP or via EUMETCast. In the case of the latter distribution mechanism, the Meteosat LSA SAF full disk is actually split into 4 geographical areas of the Meteosat disk (Figure 1) so as to reduced product file size - since many users may require data for only a part of the full disk. These four LSA SAF geographical regions are:

- Euro – Europe, covering all EUMETSAT member states;
- NAfr – Northern Africa encompassing the Sahara and Sahel regions, and part of equatorial Africa.
- SAfr – Southern Africa covering the African continent south of the Equator.

- SAmE – South American continent within the Meteosat disk.

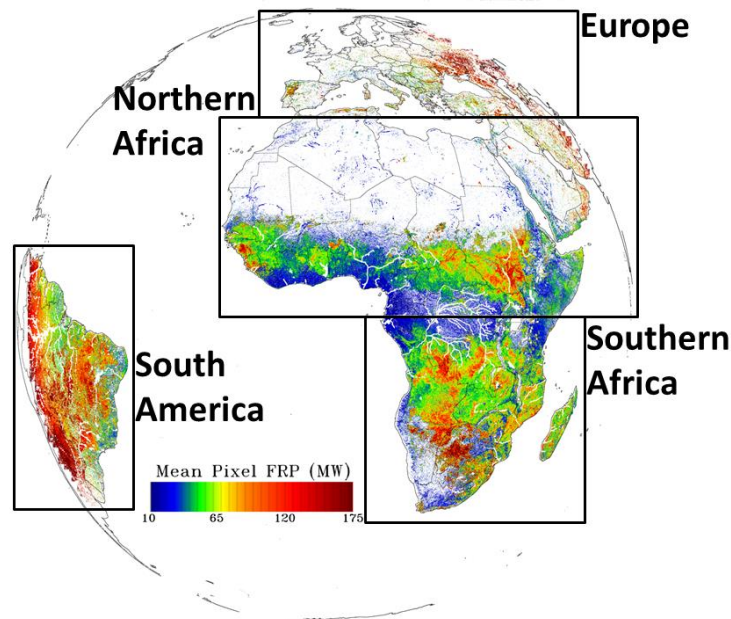


Figure 1. The Meteosat SEVIRI full disk, separated into the four individual LSA SAF geographical regions. Here the mean fire radiative power (FRP) detected in each SEVIRI pixel over a seven-year (2008-2013) period is shown. Fires are seen to be extremely widespread across sub-Saharan Africa and South America, and are also present in parts of Europe. Different regions of the Meteosat disk show different average fire characteristics, as evidenced by a wide range of mean FRP.

For all geostationary imagers, the ground pixel area increases substantially away from the sub-satellite point (SSP), in line with the increasing view zenith angle (Roberts and Wooster, 2008). This can impact derived products in different ways, and in terms of active fire detection it has the consequence of making the detection of smaller and/or lower intensity (i.e. lower FRP) fires more difficult as you move away from the SSP location, and particularly as you move towards the disk edge and the higher latitudes of the SAmE and Euro areas where the pixel areas can be 4× larger than at the SSP (Figure. 2). This effect results because the active fire detection component of the FRP-PIXEL product algorithm (the so-called Fire Thermal Anomaly algorithm, FTA described in Wooster *et al.*, 2015 and Govaerts *et al.*, 2015) is focused on the detection of sub-pixel fires, and has been shown to be able to detect fires covering down to around 10^{-4} of a SEVIRI pixel (see Roberts *et al.*, 2005; Wooster *et al.*, 2015 and EUMETSAT, 2015). This equates to a minimum detectable FRP of around 30 - 40 MW, as demonstrated therein. Since the SEVIRI pixel area increases away from the SSP, this minimum detectable pixel fraction will, in absolute terms, become a larger absolute area. Thus the minimum detectable fire size (and thus minimum detectable FRP) will also increase away from the SSP, rising to more than 4× the value at the SSP towards the disk edge. The possibility of false alarms (i.e. non-fire pixels incorrectly classified as active fires) is also simultaneously increases close to the disk edge, because of the extreme view angles involved. In particular, in the early morning

and late afternoon solar and viewing angles can conspire to cause problematic sun glints. The FTA algorithm contains many tests to avoid false alarms (see Wooster *et al.*, 2015 and Govaerts *et al.*, 2015), which are successful in identifying the vast majority (see Roberts *et al.*, 2015 and EUMETSAT, 2015), but the conditions for doing so become more challenging toward the disk edge. Hence, beyond a SEVIRI view zenith angle of 60 degrees, equivalent in Figure 2 of a nominal pixel area of ~18 km², users should expect potentially more false alarms in the LSA SAF FRP products and a substantially higher minimum FRP detection limit resulting in fewer of the real fires actually present in the region being present in the product files. The view zenith angle (PIXEL_VZA) of each detected active fire pixel is stored in the FRP-PIXEL product output files should the users wish to remove active fire detections beyond a set VZA threshold (see later descriptions of file contents).

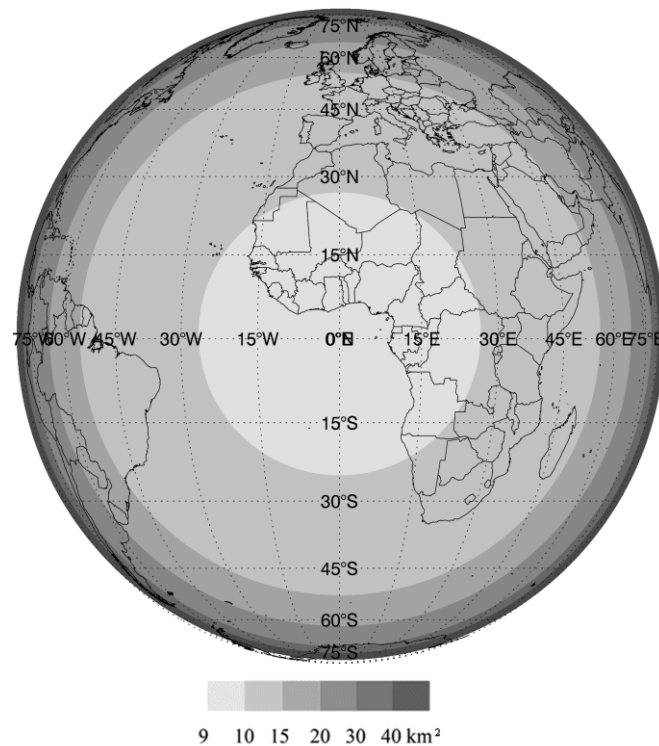


Figure 2. Variation of the nominal pixel area of SEVIRI (adjusted for SEVIRI oversampling). Away from the sub-satellite point the pixel area increases, with substantially larger pixel areas close to the disk edge (particularly affecting higher latitude South America and European areas). Pixels reach a nominal pixel area greater than 40 km² towards the disk edge.

The MetOp derived parameters at the LSA SAF are currently available at level 1b full spatial resolution and for the processed Product Distribution Units (PDUs), each corresponding to about 3 minutes observation. Composite and re-projected products are foreseen for a later stage of the LSA SAF. Table 1 provides a full list of LSA SAF products currently available.

Product Family	Product Group	Sensors/Platforms
Radiation	Land Surface Temperature (LST)	SEVIRI/MSG, AVHRR/Metop, FCI/MTG, VII/EPS-SG
	Land Surface Emissivity (EM)	SEVIRI/MSG, FCI/MTG (internal product for other sensors)
	Land Surface Albedo (AL)	SEVIRI/MSG, AVHRR/Metop, FCI/MTG, VII/EPS-SG, 3MI/EPS-SG
	Down-welling Short-wave Fluxes (DSSF)	SEVIRI/MSG, FCI/MTG
	Down-welling Long-wave Fluxes (DSLW)	SEVIRI/MSG, FCI/MTG
Vegetation	Normalized Difference Vegetation Index (NDVI)	AVHRR/Metop, VII/EPS-SG
	Fraction of Vegetation Cover (FVC)	SEVIRI/MSG, AVHRR/Metop, FCI/MTG, VII/EPS-SG, 3MI/EPS-SG
	Leaf Area Index (LAI)	SEVIRI/MSG, AVHRR/Metop, FCI/MTG, VII/EPS-SG, 3MI/EPS-SG
	Fraction of Absorbed Photosynthetically Active Radiation (FAPAR)	SEVIRI/MSG, AVHRR/Metop, FCI/MTG, VII/EPS-SG, 3MI/EPS-SG
	Gross Primary Production (GPP)	SEVIRI/MSG, FCI/MTG
	Canopy Water Content (CWC)	AVHRR/Metop, VII/EPS-SG
Energy Fluxes	Evapotranspiration (ET)	SEVIRI/MSG, FCI/MTG
	Reference Evapotranspiration (ET0)	SEVIRI/MSG, FCI/MTG
	Surface Energy Fluxes: Latent and Sensible (LE&H)	SEVIRI/MSG, FCI/MTG
Wild Fires	Fire Detection and Monitoring (FD&M)	SEVIRI/MSG
	Fire Radiative Power	SEVIRI/MSG, FCI/MTG, VII/EPS-SG
	Fire Radiative Energy and Emissions (FRE)	SEVIRI/MSG, FCI/MTG, VII/EPS-SG
	Fire Risk Map (FRM)	SEVIRI/MSG, FCI/MTG
	Burnt Area (BA)	AVHRR/Metop, VII/EPS-SG

Table 1. The LSA SAF Set of Products and respective sensors and platforms. The table covers both existing and future EUMETSAT satellites, and therefore refers operational products and development activities.

The LSA SAF operational processing chain is fully centralized at IPMA and is able to operationally generate, archive, and disseminate a wide set of operational products. The monitoring and quality control of the operational products, also centralized at IPMA, is performed automatically by LSA SAF software, which provides quality information that can be distributed with the products. Examples of LSA SAF products

are currently available from LSA SAF website (<http://landsaf.ipma.pt>), which also provides up to date information of development of products.

This document is one of the product user manuals (PUMs) written for LSA SAF users based on previous version (EUMETSAT, 2009). An overview of the algorithm and of the main characteristics of the FRP products generated by the LSA SAF system are described in the following sections (as well as in Wooster *et al.*, 2015). Validation information is found in the product Validation Report and Roberts *et al.*, (2015). In the Appendix we provide examples of Python code to read the FRP-PIXEL product files, and also information on how to calculate the Earth location for each SEVIRI pixel location present in either the LSA SAF geographic region file, or a full disk file (useful when working with the FRP-PIXEL Quality Product files).

2 FRP Product Purpose

The Meteosat SEVIRI Fire Radiative Power (FRP) products generated at the LSA SAF identify pixels containing fires that are actively burning at the time of a SEVIRI observation, and provide an estimate of the fires radiative power (FRP) output, together with its uncertainty. The products are delivered using an operational version of the Fire Thermal Anomaly (FTA) algorithm originally described in Roberts and Wooster (2008), but with some adjustments to cope with the requirements of an operational production chain, and also with significant enhancements to the sections deriving the FRP values of each detected fire pixel. The final operational algorithm is fully described in Wooster *et al.* (2015) and in the applicable Algorithm Theoretical Basis Document (Govaerts *et al.*, 2015).

The FRP of an active fire pixel is expressed in megawatts (MW), and represents the amount of radiant heat energy liberated per unit time from the burning vegetation and/or organic soils present within that pixel. This FRP value is related to the rate at which these fuel are being burned (as first demonstrated by Wooster *et al.*, 2005), since the radiant energy release is a direct result of the combustion process, whereby carbon-based fuel is consumed with the release of a certain “heat yield”, a fraction of which is emitted as electromagnetic radiation that can be measured with appropriate remote sensing instrumentation. Though satellite remote sensing instruments typically record electromagnetic radiation in only a part of the electromagnetic spectrum, physically-based relationships can be used to estimate the radiative emission occurring over the whole spectrum, based on the measurements made at only a limited number of wavelengths (Wooster *et al.*, 2003). A product performance evaluation for the LSA SAF FRP Products is available in the product Validation Report (also available on the LSA SAF website, and in Roberts *et al.* (2015). The latter also includes an example of product use in high spatio-temporal resolution fire emissions modelling exercise, as does Baldassarre *et al.* (2015).

The temporal integration of the FRP measured over a fire lifetime provides a measure of the total Fire Radiative Energy (FRE), which is believed proportional to the total fuel mass consumed during the combustion process. Linear relationships linking FRP, FRE and fuel consumption were first demonstrated in detail by Wooster *et al.* (2005):

Rate of biomass consumption ($\text{kg}\cdot\text{sec}^{-1}$) = $0.368(\pm 0.015)$ ·Fire Radiative Power (MW)

Equation 1

Fuel biomass combusted (kg) = $0.368(\pm 0.015)$ ·Fire Radiative Energy (MJ)

Equation 2

The FRP measure to use in Equation (1) can be taken from the SEVIRI FRP per-pixel product, whilst the FRE measure for use in Equation (2) is the integral of the FRP measured in a particular area over a certain time period (for example that which represents one particular fire event).

Once a biomass combustion rate or total is available, it can simply be multiplied by the fraction of carbon contained in the fuel (usually assumed to be ~ 50%) to estimate total carbon release, or by the standard emissions factors of different species in order to estimate the emitted mass of those species (either gases or aerosols). The standard emissions factors used in converting estimates of fuel consumption to estimates of emissions production are tabulated in, for example, Andreae and Merlet (2001) or Akagi *et al.* (2011) and any subsequent updates. An alternative approach to estimating emissions would be to directly calculate them from the FRP or FRE measurements, without the intermediate step of calculating the fuel consumption. This requires application of dedicated “radiative emissions ratios”, such as those derived for smoke aerosols by Ichoku and Kaufman (2005), and for a series of trace gases and smoke aerosols by Freeborn *et al.* (2008).

Kaiser *et al.* (2012) describe how FRP measurements made from Earth orbiting satellites are at the heart of the Global Fire Assimilation System (GFAS), which delivers fire emissions estimates to the Copernicus Atmosphere Service (CAS; www.gmes-atmosphere.eu). The Meteosat SEVIRI FRP data produced by the LSA SAF were the first geostationary FRP data to be used within this Service (Roberts *et al.*, 2015). Compared to fire emissions estimates derived from the traditional post-fire measure of burned area, emissions estimates derived from FRP measures do not require information on pre-fire fuel load or 'combustion completeness', and are available whilst the fire is still burning. They therefore offer a method to estimate the location and amount of greenhouse gas and aerosol emissions from landscape fires, as well as reactive gases (ozone precursors particularly), based directly on measures of the actual heat released from these events, and are very well suited for near-real time, operational applications related to atmospheric monitoring and forecasting.

3 Product and Algorithm description

Within the LSA SAF processing chain, the FTA algorithm is used to produce FRP data from SEVIRI at two different spatial and temporal resolutions.

The Level 2 operational **FRP-PIXEL** product contains information on pixels identified as containing actively burning fires (so-called ‘fire pixels’) at the original

SEVIRI pixel resolution every 15 minutes. The SEVIRI pixel sampling distance at the Sub Satellite Point (SSP) is nominally 3 km, and the product reports the classification of each pixel (fire pixel, non-fire pixel, cloudy pixel etc), as well as the FRP (in MW) of the detected fire pixels together with an estimate of their FRP uncertainties.

- The Level 3 operational **FRP-GRID** product provides an summary estimate of the mean FRP at 5.0° spatial resolution, averaging the total FRP measured each 1 hour interval. In addition to the FRP estimation at a coarser spatial and temporal resolution than the pixel level product provides, this Level 3 product includes statistical adjustments for presence of clouds (which can mask fires from the view of the sensor) and for undetected “small” (i.e. low FRP) fires, whose signal remains below the limit of detectability from SEVIRI. These low FRP fires can be numerous, and so they can form a significant fraction of the total FRP of an area. Refer to Section 4.3 for the limitations concerning the interpretation of this FRP-GRID product.

3.1 FRP-PIXEL Product

The estimation of FRP at a detected fire pixel requires the processing steps listed schematically below (Table 2), and are also represented graphically in Fig. 3.

The FRP-PIXEL product is generated for the full disk, and also for each of the four LSA SAF geographic regions for transmission via EUMETCAST (see Section 0).

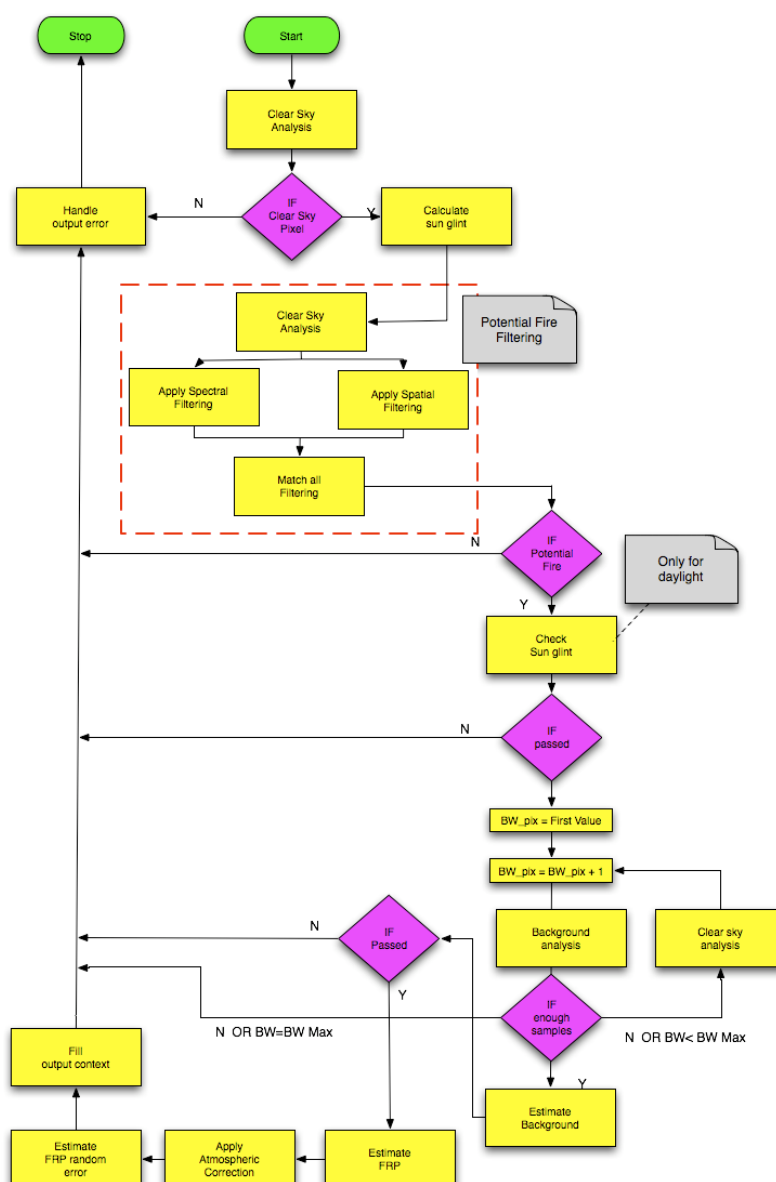


Figure 3. Flowchart illustrating the FRP-PIXEL algorithm processing steps. See Wooster et al. (2015) for a full algorithm description, or the online ATBD (Govaerts et al., 2015) available at <http://landsaf.ipma.pt>.

1	<i>Clear sky pixel identification:</i>	Identification of the clear sky pixels. A cloud mask together with some conditions on the radiance and ratio of the input channels are used for this purpose (see ATBD Section 3.3).
2	<i>Potential fire detection:</i>	Detection, using spectral and spatial filtering of the potential fire pixels (see ATBD Section 3.4).
3	<i>Background identification:</i>	Identification and estimation of the pixel background radiance. A square window region ranging in size from 5x5 to 15x15 pixels surrounding the potential fire is analysed according to a set of conditions on both brightness temperature and radiance (see ATBD Section 3.5).
4	<i>FRP assessment at pixel level:</i>	Estimation of the FRP for the potential fire pixels. It is proportional to the middle infrared radiance difference between the potential fire pixel and the mean radiance of the background window in the 3.9 μm channel (see ATBD Section 3.6)
5	<i>Apply Atmospheric correction</i>	Apply a correction to account for fire signal attenuation due to the atmosphere (see ATBD Section 3.6).
6	<i>FRP uncertainty assessment</i>	The random error in FRP retrieval is estimated using the standard error propagation formula (see ATBD Section 3.7)
7	<i>Detection confidence estimation:</i>	A value between 0 and 1 is assigned to each detected fire pixel. Higher values correspond to higher detection confidences (which are typically higher FRP fire pixels). As explained in the Product User Manual (PUM) the SEVIRI FRP-PIXEL product confidently detects active fire pixels whose FRP exceeds $\sim 30 \text{ MW}$.

Table 2. FRP-PIXEL processing steps, see Wooster *et al.* (2015) for more details.

3.1.1 Inputs

The dynamic input files used to generate the FRP-PIXEL products are:

<i>SEVIRI Radiance 0.6 μm</i>	mandatory	- Residual cloud screening
<i>SEVIRI Radiance 3.9 μm</i>	mandatory	- Residual cloud screening - Potential fire pixel assessment - Background window assessment - FRP estimation
<i>SEVIRI Radiance 10.8 μm</i>	mandatory	- Residual cloud screening - Potential fire pixel assessment - Background assessment
<i>SEVIRI Radiance 12.0 μm</i>	mandatory	- Residual cloud screening - Potential fire pixel assessment - Background assessment
<i>Cloud Mask from the NWC SAF</i>	mandatory	- Cloud screening

Total Column Water Vapour (TCVW) not mandatory - Atmospheric correction
from ECMWF

In cases where the TCVW data are not available, the processing is performed using a default value: FRP_TCWV_DEFAULT = 20 kg m⁻²

3.1.2 Outputs

The FRP-PIXEL processing chain generates two output files in HDF5 format (either for the full disk, or for each of the LSA SAF geographic regions previously cited):

- **FRP-PIXEL List Product File:** This has the format of a list, with information provided only at the locations of confirmed fire pixels having an FRP value. There is therefore one entry in the list for every fire pixel having an estimated FRP. For each fire pixel, the FRP and an exhaustive list of relevant information, such as the fire pixel background window mean temperature, is provided. The last 24 hours of the fire pixel list is also available on-line on the LSA SAF FRP Pixel Product page in KML format – which can be displayed in an application like Google Earth. This format is not archived.
- **FRP-PIXEL Quality Product File:** This has the format of a matrix whose dimensions are equal to the size of the current LSA SAF region for which the product is generated (full disk or single geographic region). For each pixel in the region, the Quality Product File provides the pixel status in relation to the fire product, i.e. whether it contains a detected fire, a cloud, was not processed etc.

The full information content of both the List and Quality Product files is described in Section 4.2 of this PUM, and in the supplement of Wooster *et al.* (2015). The FRP List Product has a small file size and it is intended for users who only need to know where and when an active fire pixel has been detected, and what the FRP and uncertainty of the fires in those pixels is estimated to be. Other users may need to know more detail, such as the reason why no fire has been detected in a specific SEVIRI pixel (e.g., cloud cover, sunglint etc) and the larger and more extensive FRP Quality Product files are available to use in this case.

3.2 FRP-GRID Product

Estimates of FRP are provided in the FRP-GRID product at a grid cell spatial resolution of 5.0° and a temporal resolution of 1 hour. The processing steps used to generate the FRP-GRID product are listed in Table 3 below.

1	<i>Total FRP at 5 degrees</i>	Summation of the FRP of all fires detected by the FRP-PIXEL product in the 5.0° box.
2	<i>Clear sky fraction</i>	Calculate the clear sky fraction of the 5.0° box. Users should multiply the total observed FRP, or the total observed FRP adjusted by the small fires factor, by this Clear sky fraction to compensate these grid cell FRP estimates for the obscuration by

		clouds present over land.
3	<i>Hourly Averaged FRP</i>	Average the FRP measured over 1 hour
4	<i>Small fires factor</i>	Store the 'small fires factor' for the grid cell. Users should multiply the total observed FRP by this region-specific adjustment factor to yield an estimate of the total FRP that might be present in the grid cell that includes the contribution from (potentially numerous) small/low intensity (i.e. low FRP) fires that are each below the SEVIRI detection limit.

Table 3. FRP-GRID processing steps, see Wooster *et al.* (2015) for more details.

Figure 4 shows an example of FRP-GRID product produced for 5 July 2015, 12:00 UTC. The total per-slot FRP recorded from fires detected in each 5 degree grid cell is reported, given as the mean FRP detected in the cell over the last hour. At this date and time, actively burning fires are primarily located in southern Africa.

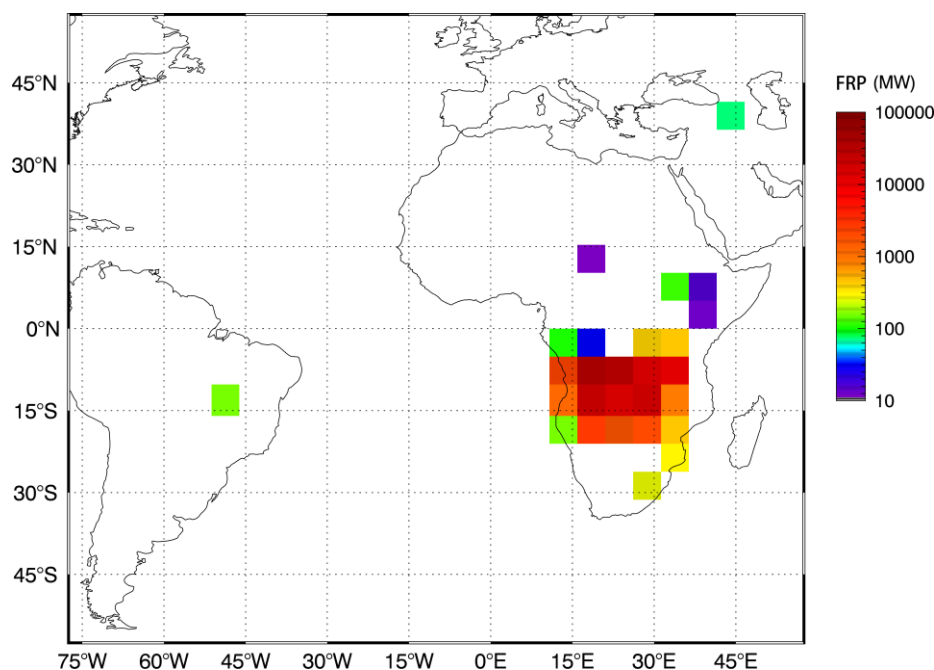


Figure 4. Example of GFRP from LSA SAF FRP-GRID product recorded on 5 July 2015, 12:00 UTC.

The FRP-GRID product is generated for the complete SEVIRI disk on a regular predefined grid – at present hourly and 5.0° as derived from consultation with users and with regard to obtaining sufficient samples with which to apply the statistically-based adjustment factors. A flowchart showing the processing executed for the estimation of the mean grid FRP is shown in Figure 5.

The default spatial and temporal domain of the FRP-GRID product is:

FRP_GRID_FIRST_LON	80 W
FRP_GRID_LAST_LON	60 E
FRP_GRID_FIRST_LAT	80 S
FRP_GRID_LAST_LAT	60 N
FRP_GRID_RESOL	5.0 degree
FRP_GRID_AGV_RANGE	1 hour

Table 4: Parameters used to define the spatial and temporal resolution of the FRP-GRID product.

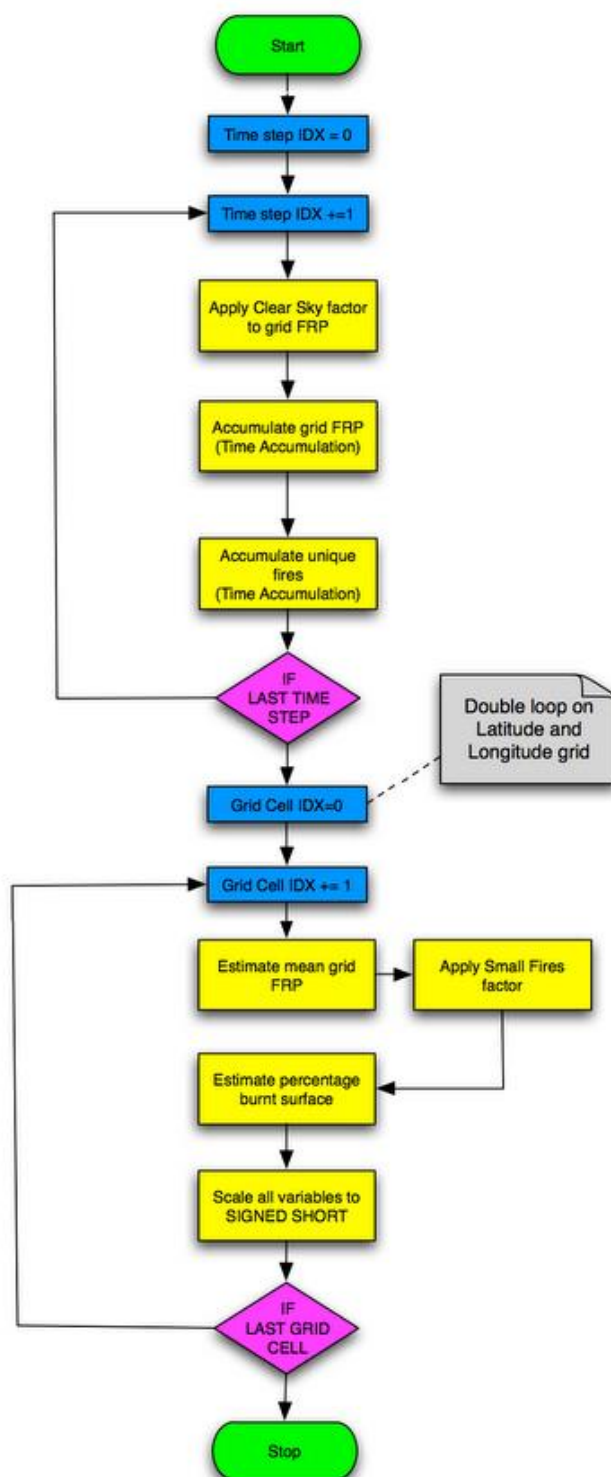


Figure 5. Flowchart showing FRP-PIXEL processing steps. See Wooster *et al.* (2015) for a full algorithm description, or online ATBD (Govaerts *et al.*, 2015).

3.2.1 Inputs

The dynamic input files needed by the FRP-GRID product are, for the complete hour:

- FRP product list generated by the FRP-PIXEL processing chain
- FRP Quality flag generated by the FRP-PIXEL processing chain
- Latitude array at pixel level (static ancillary file)
- Longitude array at pixel level (static ancillary file)

The following input is also required at the default resolution of 5 degrees.

- Small Fires adjustment Look-up table¹ (private static ancillary file)

The FRP-GRID outputs are generated even in cases where data for some regions/time-steps are missing. Specific values in the product warn the user if the lack of fires in a grid cell was due to missing inputs, or to an actual apparent absence of fires in that area. A specific field in the product also reports the number of input used for the mean temporal FRP estimation in every cell. For details refer to Section 4.3

The Latitude and Longitude ancillary files can be downloaded, like all the other public static ancillary data, from the LSA SAF web page. A “free of charge” registration is required for this service

Registration address: <https://landsaf.ipma.pt/security/login.jsp?seltab=1>

Ancillary file address: <https://landsaf.ipma.pt/auxiliarDataFiles.jsp>

3.2.2 Outputs

The output produced from the FRP-GRID processing consists of:

- FRP-Grid output file (full disk)

The coordinates of the grid are defined in degrees (see Table 4) and further product details are reported in Section 4.3

4 Output Data Description

4.1 Overview

Information on the geo-location characteristics and data distribution of the FRP products is available from the LSA SAF web-site: <http://landsaf.ipma.pt>. The FRP products are stored in HDF5 format, and have the following structure:

¹This Look-up table applies a adjustment by estimating the FRP of the low FRP fires missed by SEVIRI. For more details refers to the ATBD.

- A common set of attributes for all kinds of data, containing general information about the data (including metadata compliant with EUMETSAT U-MARF requirements);
- A dataset for the parameter values;
- Additional datasets for metadata (e.g., quality flags).

The list of global and dataset attributes is the same for all input and output files and it is detailed in the Product Output Format document (SAF/LAND/IM/POF/1.8). The HDF5 format has been developed by the National Centre for Supercomputing Applications (NCSA) at the University of Illinois. A comprehensive description is available at <http://hdf.ncsa.uiuc.edu/>.

4.2 FRP_PIXEL

At each time step the FRP_PIXEL algorithm generates two external output files named according to the following convention:

- **HDF5_LSASAF_MSG_FRP_ListProduct_<Area>_YYYYMMDDHHMM**
- **HDF5_LSASAF_MSG_FRP_QualityProduct_<Area>_YYYYMMDDHHMM**

Where <Area>, YYYY, MM, DD, HH and MM respectively denote the geographical region (MSG-Disk, Euro, NAfr, SAfr, SAme), and the year, month, day, hour and minute of data acquisition. The time specified in the filename refers to the acquisition start time for that SEVIRI image.

Previously all FRP-PIXEL products were generated separately for the smaller LSA SAF geographical regions (Euro, NAfr, SAfr, SAme), but from version 2.0 full disk (MSG-Disk) generation has also been commenced.

The Earth location of each of the pixels recorded in the FRP-PIXEL Quality Product can be calculated using the geolocation information detailed in Appendix E, which is the same as that for the other LSA SAF products. The lat/lon location of each of the individually detected active fire pixels are coded directly in the List Product.

4.2.1 Fire list product file

The FRP-PIXEL List Product File contains a list of variables available for each detected fire, as described in Table 5. Please refer to Annex C of the product ATBD (Govaerts *et al.*, 2015), or to Wooster *et al.* (2015) and its Supplement, for a detailed description of the estimation of these fields. Figure 6 shows an example of the FRP-PIXEL list product as displayed with HDFview.

VARIABLE	MEANING	UNITS	SCALE FACTOR	RANGE
FRP	Pixel FRP (with atmospheric correction applied ²). This variable contains the Fire Radiative Power estimate for the detected fire pixel.	MW	10	> 0
FRP_UNCERTAINTY	FRP random error estimate. This contains error estimate associated with retrieved FRP, derived from combination of uncertainties in FRP coefficient, fire pixel radiance, fire pixel background estimate, and atmospheric transmission. See Wooster <i>et al.</i> (2015).	MW	100	> 0
ERR_FRP_COEFF	Relative uncertainty (in the range 0 to 1) of the FRP coefficient used in the Planck Function approximation	p.n.	10000	0.1
ERR_BACKGROUND	Relative uncertainty (range 0 to 1) derived from variation in fire pixel background window	p.n.	10000	>0
ERR_ATM_TRANS	Relative uncertainty (range 0 to 1) in atmospheric transmission	p.n.	10000	>0
ERR_VERT COMP	Relative uncertainty (in the range 0 to 1) of the water vapour column total used in the atmosphere transmission	p.n.	10000	>0
ERR_RADIOMETRIC	Relative uncertainty (in the range 0 to 1) derived from the uncertainty in the fire pixel spectral radiance measure	p.n.	10000	>0
ABS_PIXEL	Pixel column number value in the SEVIRI projection	p.n.	1	[1-3712]
ABS_LINE	Pixel line number in the SEVIRI projection	p.n.	1	[1-3712]
REL_PIXEL	Pixel column number relative to the respective LSA SAF Region (only single LSA SAF geographic region products)	p.n.	1	Varying with region (unavailable in Full disk).
REL_LINE	Pixel line number relative to the respective LSA SAF Region (only single LSA SAF	p.n.	1	Varying with region (unavailable

² Applying the atmospheric correction means the per-pixel FRP based on the top-of-atmosphere radiances has been multiplied by the inverse of the field PIXEL_ATM_TRANS, whose value is also saved in the product so that it can be removed if desired.

	geographic region products)			in Full disk).
BW_NUMPIX	Number of valid pixels in the background window used for the estimation of the background temperature.	p.n.	1	[15,215]
BW_SIZE	Background window size in pixels.	p.n.	1	[5,15] ³
LATITUDE	Fire pixel centre latitude	Deg	100	[-90,90]
LONGITUDE	Fire pixel centre longitude	Deg	100	[-180,180]
FIRE_CONFIDENCE	Fire pixel confidence estimate (in the range 0 to 1)	p.n.	100	[0,1]
BT_MIR	MIR band fire pixel BT (3.9 micron)	K	10	> 0
BT_TIR	LWIR band fire pixel BT (10.8 micron)	K	10	> 0
BW_BT_MIR	Mean BT of the background window pixels in the MIR band.	K	10	> 0
BW_BTD	Mean BTD of the background window pixels (where BTD is the BT difference between MIR and LWIR channels)	K	10	> 0
PIXEL_SIZE	Pixel Area. The pixel area depends on the distance of the pixel from sub-satellite point.	km ²	100	> 9
PIXEL_VZA	View zenith angle. Estimated using real mean satellite position during acquisition of the current image.	Deg	100	[0,90]
PIXEL_ATM_TRANS	Atmospheric transmissivity in the 3.9 micron band. Used to take into account the decrease of the radiometric signal from the surface due to the atmosphere absorption.	p.n.	10000	[0,1]
ACQTIME	Pixel Acquisition Time. The ACQTIME format is HHMM. For example the time 12:14 is coded as an integer like 12x100+14 = 1214.	UTC Time	1	[0,2359]
RAD_PIX	Spectral radiance of the fire pixel in the MIR (3.9 micron) band.	MW/(m ² .s r.cm ⁻¹)	10000	>0
STD_BCK	Mean absolute deviation of MIR radiance of the background windows pixel	MW/(m ² .s r.cm ⁻¹)	10000	>0

Table 5. Information stored in the FRP-PIXEL List Product files (one value for each detected fire pixel).

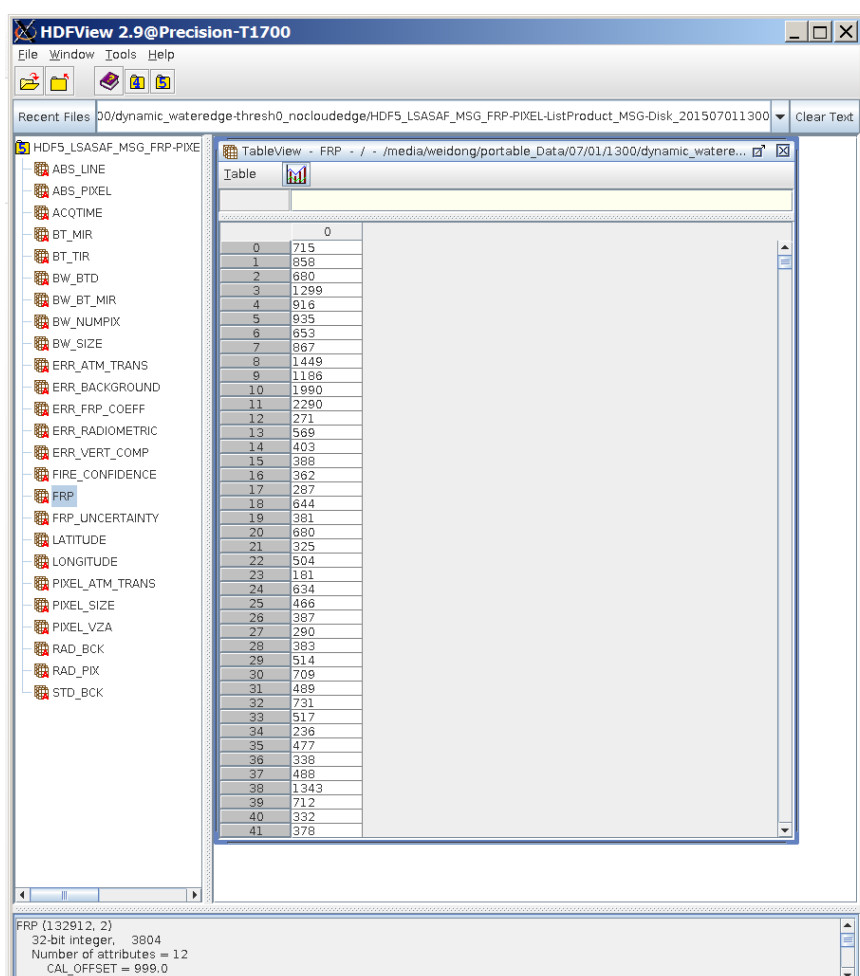
The real measured value of the variable is obtained from the values stored in the FRP-PIXEL List Product file according to the following formula:

³ Only odd values (5,7,9,...) are permitted

$$\text{Real_value} = \text{Stored_value} / \text{Scale_factor}$$

Where Stored_value is the value saved as a two byte integer in the List Product file.

REL_PIXEL and REL_LINE are pixel and line number relative to the origin of the previously defined four LSA SAF geographic regions (SAfr, NAfr, SAMer, EUro; see Figure 1). They give the coordinate of the particular fire pixel in the Quality Flag Matrix product file. Since version 2.0 of the FRP-PIXEL products the LSA SAF processing chain works on full disk products, and these two values are the same as ABS_PIXEL and ABS_LINE and are therefore no longer needed (apart from EUMETCAST transmitted files that are still delivered separately for the four LSA SAF geographic regions). ABS_PIXEL and ABS_LINE are the pixel and line number in the native SEVIRI geo-rectified Level 1.5 images.



Recent Files: 00/dynamic_watredge-thresh0_noclouedge/HDF5_LSAF_MSG_FRP-PIXEL-ListProduct_MSG-Disk_201507011300

HDF5_LSAF_MSG_FRP-PIXEL

- ABS_LINE
- ABS_PIXEL
- ACQTIME
- BT_MIR
- BT_TIR
- BW_BT_D
- BW_BT_MIR
- BW_NUMPIX
- BW_SIZE
- ERR_ATM_TRANS
- ERR_BACKGROUND
- ERR_FRP_COEFF
- ERR_RADIOMETRIC
- ERR_VERT_COMP
- FIRE_CONFIDENCE
- FRP
- FRP_UNCERTAINTY
- LATITUDE
- LONGITUDE
- PIXEL_ATM_TRANS
- PIXEL_SIZE
- PIXEL_VZA
- RAD_BCK
- RAD_PIX
- STD_BCK

Table: FRP - / - /media/weidong/portable_Data/07/01/1300/dynamic_watredge-thresh0_noclouedge/HDF5_LSAF_MSG_FRP-PIXEL-ListProduct_MSG-Disk_201507011300

Table	
0	715
1	858
2	680
3	1299
4	916
5	935
6	653
7	987
8	1449
9	1186
10	1990
11	2290
12	271
13	569
14	403
15	388
16	362
17	287
18	644
19	381
20	680
21	325
22	504
23	181
24	634
25	466
26	387
27	290
28	383
29	514
30	709
31	489
32	731
33	517
34	236
35	477
36	338
37	488
38	1343
39	712
40	332
41	378

FRP (132912, 2)
32-bit integer, 3804
Number of attributes = 12
CAL_OFFSET = 999.0

Figure 6. Example of an FRP-PIXEL List Product file structure, as viewed with HDFView. Each row in this depiction reports the FRP of a confirmed active fire pixel detected in the full disk FRP-PIXEL product being examined.

4.2.2 The FRP-PIXEL Quality Product file

This product file is a 2D array with the dimensions of the Meteosat disk (3712×3712 pixels), and contains the processing status of each SEVIRI pixel. In this file, the pixel size is the same as for the native SEVIRI images (i.e. a pixel spacing of 3 km at the sub satellite point).

VARIABLE	MEANING	UNITS	SCALE FACTOR	RANGE
QUALITY FLAG	Quality flag	N.A.	1	[0,255]

Table 6. FRP-PIXEL datasets stored as 2D matrix in the Quality Product file.

The QUALITY FLAG stored in the FRP-PIXEL Quality Product file records the processing status of all pixels in the full SEVIRI imaging disk, including active fire pixels and those where no active fire has been detected. Example code to read the FRP-PIXEL Quality Product is included in the Appendix to this Product User Manual. The Quality Product information can be very useful when comparing SEVIRI FRP products to those from other SEVIRI products or to that from other instruments, and is mandatory as input to the FRP-GRID product, where a measure of cloud cover is required in order to provide an estimate of the potential FRP obscured by cloud (at a 5 degree grid cell resolution). The coding for the QUALITY FLAG is given in Table 6.

NAME	VALUE	STATUS	REASON
FRP_APL_NOTPOT	0	FRP NOT Estimated	Not a potential fire pixel (see ATBD Section 3.4)
FRP_APL_FRP	1	FRP Estimated	Successful fire detection and FRP estimation.
FRP_APL_FRP_SAT	2	FRP Estimated	FRP estimated but with a saturated 3.9 micron channel signal. Please refer to the ATBD Section 3.6 for FRP estimation over saturated pixels.
FRP_APL_CLOUD	3	FRP NOT Estimated	The pixel is classed as cloud contaminated - fire detection was not attempted
FRP_APL_SUNG	4	FRP NOT Estimated	The pixel is classed as being affected by sun glint due to the sun-land-sensor angular condition - fire detection was not attempted.
FRP_APL_SUNGRATIO	5	FRP NOT Estimated	The SUNGRATIO test failed (see ATBD Section 3.4, Equation 30)
FRP_APL_NOBCK	6	FRP NOT Estimated	It was not possible to define the background temperature of the candidate potential fire pixel.
FRP_APL_BCKNOT	7	FRP NOT Estimated	The signal of the potential fire pixel was not sufficiently above that of the background window –

			so the pixel was not confirmed as a true fire (see ATBD Section 3.6)
FRP_APL_CLOUDEDGE	8	FRP NOT Estimated	No fire detection took place because the pixel is too close to a cloud or water edge (this class was used in previous versions of the FRP-PIXEL products, but is not used in version 2.0 onwards (i.e. since end 2015))
FRP_APL_BADINPUT	9	FRP NOT Estimated	Some input files are incomplete or corrupted .
FRP_APL_WATER	10	FRP NOT Estimated	Water body and so not processed for fire detection, introduced in version 2.0.
FRP_APL_WATEREDGE	11	FRP NOT Estimated	No fire detection took place because the pixel is close to a water body.
FRP_APL_NOTPROC	254	FRP NOT Estimated	The pixels have not been processed (i.e. they are urban, snow and ice or other non-processed pixels).
FRP_OUTSIDE_ROIS	255	FRP NOT Estimated	Celestial background (outside the full disk area, introduced in version 2.0)

Table 7. Coding flags used within the FRP-PIXEL Quality Product files.

Figure 7 shows an example FRP-PIXEL Quality Product file, derived from a full-disk SEVIRI image collected at 13:00 UTC on 5th July 2015. At left is the full disk data, whereas at right a region of south-east Africa region is shown magnified.

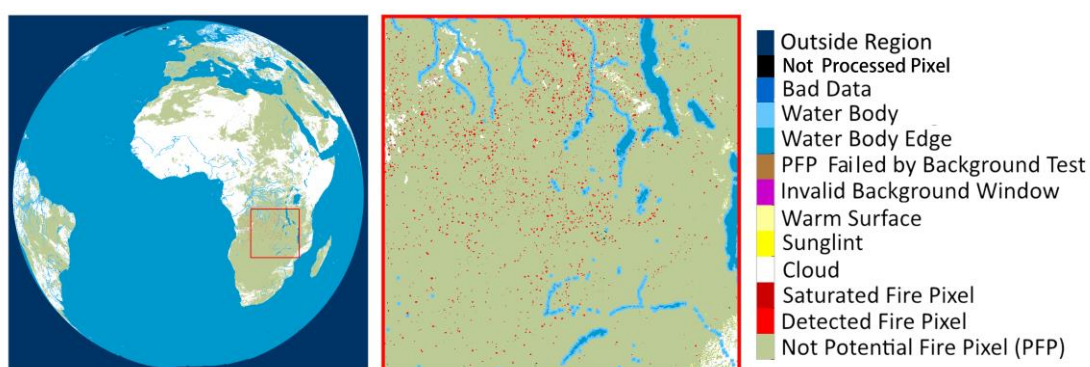


Figure 7. Example of the coding flags (Table 7) contained within the Quality Product from a SEVIRI image collected at 13:00 UTC on 5th July 2015.

The sequence of tests executed in the FTA algorithm prior to the identification of potential fire pixels is:

LAND → CLOUD → SUN GLINT

A pixel that is not classed as “land” is flagged as FRP_APL_NOTPROC (Table 7) if it is not cloud contaminated, and as FRP_APL_CLOUD if it classed as a cloud. The use of the quality indicator information is particularly important for the correct interpretation of the FRP list data given in Table 5. The following different cases can be envisaged:

- When the quality flag takes one of the following values (FRP_APL_FRP, FRP_APL_FRP_SAT) the pixel can be considered as containing an active fire, and an FRP value is estimated. From these data it is possible to estimate the combustion rate and thus the corresponding pyrogenic emission of carbon, CO₂, CO, CH₄, aerosol etc.
- When the quality flag takes the FRP_APL_NOBCK value the pixel was classed as a potential fire pixel, but it was not possible to confirm whether or not it was a true fire pixel due to an inability to estimate the average signal of the surrounding background window.
- When the quality flag takes the FRP_APL_BCKNOT value the pixel was classed as a potential fire pixel, but then was not confirmed as a true fire pixel as the pixels signal was raised insufficiently above that of the background window average.
- When the quality flag takes the FRP_APL_NOTPOT value, it means that there was no fire present in the pixel, or any fire that was present had a signal that was too weak to be detected by SEVIRI, so the pixel was not picked out as a potential fire pixel (and was thus not confirmed as a true fire pixel either). It is possible that small and/or lower intensity fires might have been present in the pixel, but they remained undetected. A statistical method is used in the FRP-GRID product to potentially account for those undetected smaller/more weakly burning (lower FRP) fires.
- When the quality flag takes one of the following values (FRP_APL_CLOUD, FRP_APL_SUNG, FRP_APL_SUNGRATIO, FRP_APL_WATEREDGE, FRP_APL_BADINPUT), it was not possible to apply the FTA active fire detection scheme due to, for instance, a sun glint condition or presence of cloud.

4.3 FRP-GRID

Every hour the FRP product processing chain generates one external FRP-GRID product output file, according to the following name convention:

- **HDF5_LSASAF_MSG_FRP_Frp_Grid_Global_YYYYMMDDSSEE**

where YYYY, MM, DD, SS and EE respectively denote the year, the month, the day, the Starting and End hour of the analysed period.

VARIABLE	MEANING	UNITS	SCALE FACTOR	RANGE
GFRP	FRP for the 5.0° grid cell, as averaged over the 1 hour period	MW	0.1	> 0
GFRP_RANGE	FRP max-min difference for the grid cell over the 1 hour period	MW	1	> 0
GRIDPIX	Number of SEVIRI pixels in the 5.0° grid cell used for the estimation of the BURNTSURF variable	p.n.	1	> 0
NUMIMG	Number of SEVIRI images used to calculate the 1 hour average of the grid cell FRP	p.n.	1	>=0
NUMFIRES	Average number of fire pixels detected in each SEVIRI image within the 5.0° grid cell during the 1 hour period	p.n.	100	>= 0
BURNTSURF	Percentage of individual grid cell pixels having had a fire detected within them during the 1 hour period	p.n.	100	[0,100]
LATITUDE	Grid cell latitude (centre of the current grid cell)	Deg	100	[-90,90]
LONGITUDE	Grid cell longitude (centre of the current grid cell)	Deg	100	[-180,180]
GFRP_CLOUD_CORR	Factor enabling accounting for the cloud cover of the 5.0° grid cell, averaged over 1 hour (1 means cloud free)	p.n.	100	[0,1]
ATMTRANS	Mean atmospheric transmittance of the 5.0° grid cell calculated over the 1 hour period	p.n.	10000	[0,1]
GFRP_ERROR	Total error associated with GFRP taking into account FRP_UNCERTAINTY in the pixel level product, as well as the errors associated with the region-specific adjustment factors.	MW	1	>0
GFRP_ERR_FRP	Error in GRP attributed solely to FRP_UNCERTAINTY values held in the pixel level product	MW	1	>0
GFRP_QI	Quality indicator associated with the estimation of GFRP	p.n	100	[0,1]

Table 8. Datasets stored within the FRP-GRID products as a 2D matrix.

The real measured values of the variables stored in the FRP-GRID product are obtained using the following formula:

$$\text{Real_value} = \text{Stored_value} / \text{Scale_factor}$$

Where the Stored_value is the value saved as a two byte integer in the dataset.

The FRP-GRID product also includes the information about the reason why no fires have been found. The two possible reasons, “input data missing” and “no detected fire in the grid cell”, are coded in the product as follows:

- Input Data Missing: 32767⁴
- No Fires in the Grid Cell: 0

As already discussed, the FRP-PIXEL product allows pyrogenic emissions estimation for those fires which have been successfully detected, but suffers from some limitations due to the obscuring presence of meteorological clouds, and from the non-detection of ‘small’ and/or low intensity (i.e. low FRP) fires due the relatively coarse pixel size of SEVIRI. For cases where meteorological clouds are covering significant fires, and/or where there are significant numbers of undetected low-FRP fire pixels, the true pyrogenic emissions may well be underestimated when based solely on the observed FRP. This then might lead to significant biases when integrated over a long time period or a large area.

To circumvent these limitations, the FRP-GRID product contains information that can be used to make adjustments for the fraction of the grid cell that is cloudy, and therefore where no fire detection could take place. It also contains an adjustment for the low FRP fires that are under-detected by SEVIRI. See Wooster *et al.* (2015) for details. Importantly the observed FRP is also obtainable from this product (i.e. the value without these corrections applied) should the user require it. These corrections are statistical and aim at reducing the impact of these two issues (cloud cover and “missing” low FRP fires whose FRP is below the SEVIRI detection limit), and is performed at a sub-continental scale and over a longer period of time than one SEVIRI imaging slot. Specifically, the adjustments that compensate for the undetected FRP are intended to provide an estimate of the FRP that would have been measured by MODIS in the centre two-thirds of its swath (i.e. where MODIS makes the most accurate measures of landscape scale fires and their FRP; see Freeborn *et al.*, 2011). In this way the GFRP values stored in the FRP-GRID product are aimed to be representative of the near-nadir response of MODIS. The adjustment factor applied available in the GFRP product does not account for the temporal variability in the SEVIRI-to-MODIS ratios of FRP that are induced by diurnal and seasonal fluctuations in fire activity (Freeborn *et al.*, 2009). The use of a different adjustment factor for each of the four LSA SAF geographic regions, however, does address the broad spatial differences in the sensor-to-sensor relationships that potentially arise from (i) differences in fire regimes, and (ii) differences in SEVIRI view zenith angle across the full SEVIRI disk. Also note that the adjustment factors were developed with the specific purpose of providing unbiased estimates of the instantaneous FRP that MODIS would have

⁴The value saved for the “input data missing” case is the Maximum Signed Short Integer value. The products are all scaled as signed short.

measured within a 5.0° grid cell. Thus the adjustment factors are only statistically valid when emissions estimates are integrated over this spatial resolution.

In terms of the information contained within the product, the GFRP value in the FRP-GRID product is the hourly mean FRP measure recorded in the grid cell, with the statistical correction for undetected small fires applied (the regionally-varying multiplier stored in GFRP_CLOUD_CORR for each grid cell and explained in the product ATDB is used for the adjustment). The cloud adjusted GFRP value can be calculated by multiplying the GFRP value by GFRP_CLOUD_CORR value stored at each grid cell. If users wish to remove the "small fires adjustment" and just use the observed mean FRP values they can divide GFRP by the small fire correction factors reported for each LSA SAF geographic region in the Appendix of the product ATBD (available at <http://landsaf.ipma.pt>).

It must also be remembered that MODIS itself is likely to miss a proportion of the most weakly burning events. It is not possible to identify the location of an undetected fire within a 5.0° grid cell, nor is it appropriate to apply an adjustment factor to an individual fire event. In addition, due to the right-skewed distributions of FRP measured across the landscape (i.e. the relative abundance of lower FRP fire pixels compared to higher FRP fire pixels, but also the 'long tail' of higher FRP fire pixels), the adjustment factors applied at 5.0° grid cell resolution and hourly temporal resolution tend to underpredict the FRP that would have been measured by MODIS at regional and weekly scales. An evaluation of these region-specific biases can be found in the LSA SAF FRP Product Validation Report (available on the LSA SAF website and in Roberts *et al.*, 2015).

In summary, the use of the FRP-PIXEL product is appropriate for the study and emissions estimation of individual fires but, as outlined above, this product suffers from the effects of cloud cover and undetected smaller (lower FRP) fires. In turn, the FRP-GRID product maybe more appropriate for emission estimation over longer time periods at more regional scales, but is not suitable for the estimation of emissions of individual fires.

4.4 FRP-PIXEL Product Accuracy and Product Uncertainty

The theoretical and radiative transfer modelling analysis of the FRP algorithm performance has shown that the MIR radiance method algorithm used within the SEVIRI LSA SAF FRP product has an underlying accuracy of $\pm 12\%$ over the temperature range expected for actively burning open vegetation fires, and that the assumptions made when implementing this algorithm on data of highly-sub pixel sized fires (as will be the case with coarse spatial resolution satellite data such as that from SEVIRI) in theory introduce negligible other errors (Wooster *et al.*, 2005). In this case, if the fire pixels that comprise an individual fire can be reliably detected, show a sufficiently large MIR radiance increase above the background, and if the MIR atmospheric transmission is reliably known, then the FRP can be quantified to around this level of uncertainty. Differences between the original KCL algorithm (Roberts and Wooster, 2008) and the LSA SAF implementation are negligible in this respect.

In practical terms, the most limiting factor for product accuracy appears to be the current relatively coarse pixel size of SEVIRI at the sub-satellite point, which further increases near the disk edge (Figure 2). As detailed in the product validation report (VR) and in Roberts *et al.* (2015), most fire pixels with FRP values less than ~ 30 MW probably escape detection by SEVIRI even at the SSP, and fires with FRP close to this will likely be undercounted because the enhancement of the MIR signal due to the fire with respect to the (somewhat variable) background window signal is rather small and thus difficult to identify conclusively. MODIS for example can reasonably reliably detect fire pixels with an FRP of ~ 8 MW burning close to the centre of its swath at the time of the Terra or Aqua satellite overpass, because it has a nadir pixel area around an order of magnitude lower than SEVIRI at the SSP (1 km²), though towards the MODIS swath edge MODIS pixels become similar in area to those of the SEVIRI SSP. As discussed in Section 1, the SEVIRI minimum FRP detection limits also increase away from the SSP, and become very large towards the disk edge where product performance is degraded substantially. Users may therefore wish to ignore results from active fire pixels with view zenith angles larger than ~ 60 °, as explained in the Introduction (Section 1). Users should also note that because the enhancement of the MIR signal due to a fire with respect to the (somewhat variable) background window signal is smaller and thus more difficulty to precisely measure at lower FRP fire pixels, the absolute value of the FRP uncertainty metric (FRP_UNCERTAINTY) present in the FRP-Pixel List Product file is generally higher for lower FRP fire pixels.

To some extent, the impacts of the coarse spatial resolution of SEVIRI in terms of fire pixel underdetection are balanced by the extremely high temporal resolution of the geostationary observations. As was shown for fires in the Central African Republic (Wooster *et al.*, 2015), over the course of a day SEVIRI will capture a signal from most of the fire events that the much higher spatial resolution MODIS instruments on EOS Aqua and Terra can detect during their four-times per day overpasses. This is related to the ability of SEVIRI to observe the complete fire life cycle, and thus capture fires when they reach their peak intensity even if they are not detected at other times in their life cycle. However, for any particular SEVIRI observation, the cumulative FRP measured at the regional scale (e.g. grid cell or country-scale) is likely to be an underestimate of what would have been measured by MODIS had it observed the whole area at that same moment, because of SEVIRI's inability to detect the lowest FRP fire pixels.

Due to the higher spatial resolution observations and wide usage of the MODIS active fire products (Giglio *et al.*, 2003), these are taken to be the reference standard against which the SEVIRI FRP product has been assessed. MODIS-to-SEVIRI matchups are identified on a 'per fire cluster' basis, a matched cluster representing a set of spatially close or contiguous fire pixels seen in both imagers at the same time (though there maybe different numbers of pixels in the MODIS representation than the SEVIRI representation for example). Matchup results shown in the product Validation Report (<http://landsaf.ipma.pt>), show the FRP-PIXEL product meets its Target Accuracy, with 79% of the SEVIRI-to-MODIS fire-cluster matchups having an FRP difference less than 50%. Furthermore, 62% of them having an FRP difference less than 30%, and 53% less than 20%. There is also minimum bias seen between the two measures,

indicating that SEVIRI provides an unbiased estimate with respect to MODIS when both see the same fires at the same time.

However, at the regional scale, errors of active fire detection with respect to MODIS are high when both SEVIRI and MODIS view the same area at the same time, with SEVIRI missing more than half of the fire pixels on average – since most regions are usually dominated by low FRP fires. This leads to regional scale underestimation by SEVIRI due to its failure to detect these lowest FRP fires. See Roberts *et al.* (2015) and the LSA SAF FRP Product Validation Report for further details. Furthermore, since the MIR channel on SEVIRI was not designed for fire detection but rather primarily for cloud and land surface monitoring, it saturates around 335 K, a pixel integrated brightness temperature that could be exceeded by larger fire events. The effect of this saturation would be an underestimation of FRP for very high FRP fires, and thus a consistent bias, so instead at such pixels an estimate of the unsaturated FRP is provided within the FRP products with an appropriately increased uncertainty. For more information please refer to the FRP Product Validation Report (<http://landsaf.ipma.pt>) and to Wooster *et al.* (2015) and Roberts *et al.* (2015).

4.5 Summary of Product Characteristics

Product Name:	Fire Radiative Power
Product Code:	FRP (Fire Radiative Power)
Description of Product:	Estimation of the Fire Radiative Power of pixels identified as containing actively burning fires
Coverage:	MSG full disk (Land pixels)
Units	MW
Product Level FRP-PIXEL:	Level 2
Packaging:	Full Disk (and also Euro; NAfr; SAfr; SAME)
Resolution:	Spatial: SEVIRI full resolution (3 km sampling distance at the sub-satellite point)
Generation:	every 15 min
Uncertainty:	~ 80% of per-fire FRP within $\pm 50\%$ of MODIS value
Product Size:	List Fire Product ~20 Kb ⁵ Quality Matrix ~ 4.3 Mb

Region	Uncompressed	Compressed
--------	--------------	------------

⁵ The actual size depends on the number of detected fires.

HDF5_LSASAF_MSG_FRP_ListProduct_<Area>_YYYYMMDDHHMM		
MSG-Disk	20 - 350 Kb	10 – 150 Kb
Euro	6 - 35 Kb	1 – 3 Kb
NAfr	6 - 40 Kb	1 – 10 Kb
SAfr	6 - 40 Kb	1 – 29 Kb
SAme	6 - 40 Kb	1 – 4 Kb
HDF5_LSASAF_MSG_FRP_QualityProduct_<Area>_YYYYMMDDHHMM		
MSG-Disk	53 Mb	250 – 350 Kb
Euro	4.3 Mb	41 – 67 Kb
NAfr	9.8 Mb	102 – 156 Kb
SAfr	5.6 Mb	51 – 111 Kb
SAme	4.1 Mb	35 – 63 Kb

Table 9: Compressed and uncompressed size of the two FRP-PIXEL output files generated for the full disk and also separately for each LSA SAF geographic region.

Product Level FRP-GRID: Level 3
Packaging: MSG SEVIRI full disk (Land pixels)
Resolution: Spatial: 5 degree (112 km × 112 km at the Equator)
Generation: every hour
Accuracy
Product Size: Grid Product ~ uncompressed: 850 Kb

5 References

Akagi, S. K., Robert J. Yokelson, C. Wiedinmyer, M. J. Alvarado, J. S. Reid, T. Karl, J. D. Crounse, and P. O. Wennberg (2011) Emission factors for open and domestic biomass burning for use in atmospheric models. *Atmos. Chem. Phys.*, 9, 4039-4072

Andreae, M. O. and Merlet P. (2001) Emission of trace gases and aerosols from biomass burning, *Global Biogeochem. Cycles*, 15, 955–966.

Baldassarre, G., L. Pozzoli, C. C. Schmidt, A. Unal, T. Kindap, W. P. Menzel, S. Whitburn, P-F. Coheur, A. Kavgaci, and J. W. Kaiser (2015) Using SEVIRI fire observations to drive smoke plumes in the CMAQ air quality model: a case study over Antalya in 2008, *Atmos. Chem. Phys.*, 15, 8539-8558.

Dickinson R.E (1983) Land surface processes and climate – Surface albedos and energy balance, *Adv. Geophys.*, 25, 305-353.

EUMETSAT (2008) SAF for Land Surface Analysis: Validation Report FRP. SAF for Land Surface Analysis, Report SAF/LAND/IM/VR FRP/I 08, 114p.

EUMETSAT (2009) Fire Radiative Power Product User Manual. Technical Report SAF/LAND/IM/PUM FRP/1.1, EUMETSAT.

EUMETSAT (2015) SAF for Land Surface Analysis: Validation Report FRP. SAF for Land Surface Analysis, Report SAF/LAND/IM/VR FRP/II 10, 40p.

Ferranti, L. e P. Viterbo (2006) The European Summer of 2003: Sensitivity of Soil Water Initial Conditions. *J. Climate*, 19, 3659-3680.

Freeborn, P.H., Wooster, M.J., Hao, W.M., Ryan, C.A., Nordgren, B.L. Baker, S.P. and Ichoku, C. (2008) Relationships between energy release, fuel mass loss, and trace gas and aerosol emissions during laboratory biomass fires, *J. Geophys. Res.*, Vol. 113, No. D1, D01102, 10.1029/2007JD008489

Freeborn, P. H., Wooster, M. J., Roberts, G., Malamud, B. D., & Xu, W. (2009). Development of a virtual active fire product for Africa through a synthesis of geostationary and polar orbiting satellite data. *Remote Sens. Environ.*, 113(8), 170

Freeborn, P. H., Wooster, M. J. and Roberts, G. (2011). Addressing the spatiotemporal sampling design of MODIS to provide estimates of the fire radiative energy emitted from Africa. *Remote Sens. Environ.*, 115(2), 475-489.

Govaerts, Y.M. Wooster M. Lattanzio A., Roberts G. (2009) MSG SEVIRI Fire Radiative Power (FRP) characterization Algorithm Theoretical Basis Document Version 2.2, Report No EUM/MET/SPE/06/0398, 2009

Govaerts, Y.M. Wooster, Roberts, G., Freeborn, P., XU, W., He, J. and Lattanzio A (2015) MSG SEVIRI Fire Radiative Power (FRP) characterization Algorithm Theoretical Basis Document Version 2.8 , Report No EUM/MET/SPE/06/0398, 2015

Ichoku, C. and Kaufman Y. J. (2005) A method to derive smoke emission rates from MODIS fire radiative energy measurements, *IEEE Trans. Geosci. Remote Sens.*, 43(11), 2636– 2649.

Kaiser, J. W., A. Heil, M. O. Andreae, A. Benedetti, N. Chubarova, *et al.* (2012) Biomass burning emissions estimated with a global fire assimilation system based on observed fire radiative power, *Biogeosciences*, 9, 527-554.

Mitchell, K., *et al.*, 2004: The multi-institution North American Land Data Assimilation System NLDAS: Utilizing multiple GCIP products and partners in a continental distributed hydrological modeling system, *J. Geophys. Res.*, 109, doi:10.1029/2003JD003823.

Roberts, G. and Wooster, M.J. (2007) New Perspectives on African Biomass Burning Dynamics, *EOS Tras. AGU*, 88, 369-270.

Roberts, G., Wooster, M.J., Perry, G.L.W., Drake, N., Rebelo, L-M., Dipotso, F. 2005. Retrieval of biomass combustion rates and totals from fire radiative power observations: application to southern Africa using geostationary SEVIRI Imagery. *J. Geophys. Res.*, 110, doi: 10.1029/2005JD006018.

Roberts, G.J. and Wooster, M.J (2008) Fire Detection and Fire Characterization Over Africa Using Meteosat SEVIRI, *IEEE Trans on Geosci. and Remote Sens.*, 46, doi: 10.1109/TGRS.2008.915751

Roberts, G., Wooster, M. J., Xu, W., Freeborn, P. H., Morcrette, J.-J., Jones, L., Benedetti, A., Jiangping, H., Fisher, D., and Kaiser, J. W. (2015) LSA SAF Meteosat FRP products – Part 2: Evaluation and demonstration for use in the Copernicus Atmosphere Monitoring Service (CAMS), *Atmos. Chem. Phys.*, 15, 13241-13267, doi:10.5194/acp-15-13241-2015, 2015.

Schmetz, J., P. Pili, S. Tjemkes, D. Just, J. Kerkman, *et al.* (2002), An introduction to Meteosat Second Generation (MSG), *Bull. Amer. Meteor. Soc.*, 83, 977-992.

Wooster, M. J., G. Roberts, G. L. W. Perry, and Y. J. Kaufman, 2005, Retrieval of biomass combustion rates and totals from fire radiative power observations: FRP derivation and calibration relationships between biomass consumption and fire radiative energy release, *J. Geophys. Res.*, 110, D24311, doi:10.1029/2005JD006318.

Wooster, M. J., Roberts, G., Freeborn, P. H., Xu, W., Govaerts, Y., Beeby, R., He, J., Lattanzio, A., Fisher, D., and Mullen, R. (2015). LSA SAF Meteosat FRP products – Part 1: Algorithms, product contents, and analysis. *Atmos. Chem. Phys.*, 15, 13217-13239, doi:10.5194/acp-15-13217-2015, 2015.

6 Developers

Responsible: Martin Wooster (King's College London)

Contributors:

EUMETSAT

Germany

Yves M. Govaerts
Alessio Lattanzio

IPMA

Portugal

Isabel Trigo
Sandra Coelho
Carla Barroso

King's College London

U.K.

Jiangping He
Weidong Xu
Gareth Roberts
Patrick Freeborn

Appendix A. Product Metadata – SEVIRI FRP

Attribute	Allowed Values	Data Type
SAF	LSA	String<3>
CENTRE	IM-PT	String<5>
ARCHIVE_FACILITY	IM-PT	String<5>
PRODUCT	FRP	String<79>
PARENT_PRODUCT_NAME	Cma, TCWV, Brightness Temperature	Array(4) of string<79>
SPECTRAL_CHANNEL_ID	768	Int
PRODUCT_ALGORITHM_VERSION	X.Y	String<4>
CLOUD_COVERAGE	NWC-CMa,	String<20>
OVERALL_QUALITY_FLAG	OK or NOK	String<3>
ASSOCIATED_QUALITY_INFORMATION	-	String<511>
REGION_NAME	One of: MSG-Disk, Euro, NAfr, SAfr, SAm	String<4>
COMPRESSION	0	Int
FIELD_TYPE	Product	String<255>
FORECAST_STEP	0	Int
NC	REGION_NAME dependent	Int
NL	REGION_NAME dependent	Int
NB_PARAMETERS	2	Int
NOMINAL_PRODUCT_TIME	YYYYMMDDhhmmss	String<14>
SATELLITE	MSGX	Array[10] of String<9>
INSTRUMENT_ID	SEVI	Array [10] of String<6>
INSTRUMENT_MODE	STATIC_VIEW	String<511>
IMAGE_ACQUISITION_TIME	YYYYMMDDhhmmss	String<14>
ORBIT_TYPE	GEO	String<3>
PROJECTION_NAME	Geos<sub_Ion>	String<15>
NOMINAL_LONG	Actual Satellite Nominal Longitude	Real
NOMINAL_LAT	Actual Satellite Nominal Latitude	Real
CFAC	13642337	Int

Attribute	Allowed Values	Data Type
LFAC	13642337	Int
COFF	REGION_NAME dependent	Int
LOFF	REGION_NAME dependent	Int
START_ORBIT_NUMBER	0	Int
END_ORBIT_NUMBER	0	Int
SUB_SATELLITE_POINT_START_LAT	0.0	Real
SUB_SATELLITE_POINT_START_LON	0.0	Real
SUB_SATELLITE_POINT_END_LAT	0.0	Real
SUB_SATELLITE_POINT_END_LON	0.0	Real
SENSING_START_TIME	YYYYMMDDhhmmss	String<14>
SENSING_END_TIME	YYYYMMDDhhmmss	String<14>
PIXEL_SIZE	3.1km	String<10>
GRANULE_TYPE	DP	String<2>
PROCESSING_LEVEL	02	String<2>
PRODUCT_TYPE	LSAFRP	String<8>
PRODUCT_ACTUAL_SIZE	Depends on the region	Integer > 0, encoded as String<11>
PROCESSING_MODE	N	String<1>
DISPOSITION_FLAG	O	String<1>
TIME_RANGE	15-min	String<20>
STATISTIC_TYPE	-	String<20>
MEAN_SSLAT	REGION_NAME dependent	Real
MEAN_SSLON	REGION_NAME dependent	Real
PLANNED_CHAN_PROCESSING	0	Integer
FIRST_LAT	0	Real
FIRST_LON	0	Real

Table A 1: General attributes of the files for the SEVIRI FRP product. Regionally varying parameters are listed in Table A 5.

Attribute	Description	Data Type
-----------	-------------	-----------

CLASS	Data	String, length=4
PRODUCT	FRP	String, length=3
PRODUCT_ID	235	32-bit integer
N_ COLS	Depend on REGION_NAME	32-bit integer
N_ LINES	Depend on REGION_NAME	32-bit integer
NB_BYTES	2	32-bit integer
SCALING_FACTOR	100.0	64-bit floating-point
OFFSET	0.0	64-bit floating-point
MISS_VALUE	-8000	32-bit integer
UNITS	Degrees Celsius	String, length=15
CAL_SLOPE	999.0	64-bit floating-point
CAL_OFFSET	999.0	64-bit floating-point

Table A 2: Attributes of the FRP/SEVIRI dataset.

Attribute	Description	Data Type
CLASS	Data	String, length=4
PRODUCT	Q_FLAGS	String, length=7
PRODUCT_ID	999	32-bit integer
N_ COLS	Depend on REGION_NAME	32-bit integer
N_ LINES	Depend on REGION_NAME	32-bit integer
NB_BYTES	2	32-bit integer
SCALING_FACTOR	1.0	64-bit floating-point
OFFSET	0.0	64-bit floating-point
MISS_VALUE	-9999	32-bit integer
UNITS	Dimensionless	String, length=13
CAL_SLOPE	999.0	64-bit floating-point
CAL_OFFSET	999.0	64-bit floating-point

Table A 3: Attributes of the FRP/SEVIRI Quality Flag information dataset.

FRP Code details

The list of error codes generated by the FRP_PIXEL algorithm is listed in Table A 4. In case of fatal errors, the FRP_PIXEL process aborts.

ERROR CODE	MESSAGE
FRP_NOERROR	Processing :No Error
FRP_PDL_FILE_OPEN_ERROR	Fatal Error: File Open
FRP_PDL_IMGLINEHDRREAD_ERROR FRP_PDL_IMGLINEREAD_ERROR FRP_PDL_READDAM_ERROR FRP_PDL_READ_ERROR	Fatal Error: File Read
FRP_PDL_FILEWRITE_ERROR	Fatal Error: File Write
FRP_PDL_ALLOC_ERROR	Fatal Error: Memory Allocation

Table A 4: FRP_PIXEL algorithm fatal errors

Appendix B. Exemplar Python code to read FRP-PIXEL files.

```
import h5py,os,sys
import numpy as np

def get_h5_dataset(f, dsname):
    ds = dsname in f
    if ds:
        ds = f[dsname]
        d = ds[:]
        missing = ds.attrs.get("MISSING_VALUE")
        if missing is not None:
            mask = (d == missing)
            scale = ds.attrs.get("SCALING_FACTOR")
            offset = ds.attrs.get("OFFSET")
            if (scale is not None) and (offset is not None):
                d = d/scale + offset
            if missing is not None:
                d[mask] = np.nan
        return d
    else:
        f.close()
        print 'can not find dataset: "%s" in hdf5 file'%(dsname)
        sys.exit('UNABLE_TO_PROCESS')

def read_lsasaf_h5(inputfiles):
    data = { }
    print '-'*80
    for f in inputfiles:
        path, filename = os.path.split(f)
        info = filename.split('_')
        print filename
        t = info[5]
        k = info[3]
        try:
            fh = h5py.File(f, "r")
        except:
            print 'not a valid hdf5 file: ',
            sys.exit('INPUT_NOT_FOUND')
        else:
            if k == 'FRP-PIXEL-ListProduct':
                ds = ['LONGITUDE', 'LATITUDE', 'FRP', 'ACQTIME', 'PIXEL_VZA']
            elif k == 'FRP-PIXEL-QualityProduct':
                ds = ['QUALITYFLAG']
            elif k == 'FTA-FRP':
                ds = ['GFRP','LATITUDE','LONGITUDE']
            elif k == 'LAT' or k == 'LON':
                t='static'
```

```
        ds = [k]
    else:
        continue
    if t not in data:
        data[t] = {}
    for d in ds:
        data[t][d] = get_h5_dataset(fh, d)
    fh.close()
return data

if __name__ == "__main__":
    user_home = os.environ['HOME']
    in_root = user_home + '/data/'
    filename = in_root + 'HDF5_LSASAF_MSG_FRP-PIXEL-ListProduct_MSG-Disk_201507311300'
    dt = read_lsasaf_h5([filename])
    FRP=np.flipud(dt['201507311300']['FRP'])
```

Appendix C. Geolocation/Rectification.

The FRP-PIXEL Quality Product information is generated pixel-by-pixel, maintaining the original resolution of SEVIRI level 1.5 data. These correspond to rectified images to 0° longitude, which present a typical geo-reference uncertainty of about 1/3 of a pixel. Data are kept in the native geostationary projection.

Files containing the latitude and longitude of the centre of each pixel may be downloaded from the Land-SAF website (<http://landsaf.ipma.pt>; under “Static Data and Tools”):

Longitude

HDF5_LSASAF_MSG_LON_Euro_4bytesPrecision.bz2
HDF5_LSASAF_MSG_LON_NAfr_4bytesPrecision.bz2
HDF5_LSASAF_MSG_LON_SAfr_4bytesPrecision.bz2
HDF5_LSASAF_MSG_LON_SAm_e_4bytesPrecision.bz2
HDF5_LSASAF_MSG_LON_MSG-Disk.bz2

Latitude

HDF5_LSASAF_MSG_LAT_Euro_4bytesPrecision.bz2
HDF5_LSASAF_MSG_LAT_NAfr_4bytesPrecision.bz2
HDF5_LSASAF_MSG_LAT_SAfr_4bytesPrecision.bz2
HDF5_LSASAF_MSG_LAT_SAm_e_4bytesPrecision.bz2
HDF5_LSASAF_MSG_LAT_MSG-Disk.bz2

Alternatively, since the data are in the native geostationary projection, centred at 0° longitude and with a sampling distance of 3 km at the sub-satellite point, the latitude and longitude of any pixel may be easily estimated. Given the pixel column number, $ncol$ (where $ncol=1$ correspond to the westernmost column of the file), and line number, $nlin$ (where $nlin=1$ correspond to the northernmost line), the coordinates of the pixel may be estimated as follows:

$$lon = \arctg\left(\frac{s_2}{s_1}\right) + sub_lon \quad \text{longitude (deg) of pixel centre}$$

$$lat = \arctg\left(p_2 \cdot \frac{s_3}{s_{xy}}\right); \quad \text{latitude (deg) of pixel centre}$$

where

sub_lon is the sub-satellite point ($sub_lon=0$)

and

$$s_1 = p_1 - s_n \cdot \cos x \cdot \cos y$$

$$s_2 = s_n \cdot \sin x \cdot \cos y$$

$$s_3 = -s_n \cdot \sin y$$

$$s_{xy} = \sqrt{s_1^2 + s_2^2}$$

$$s_d = \sqrt{(p_1 \cdot \cos x \cdot \cos y)^2 - (\cos^2 y + p_2 \cdot \sin^2 y) \cdot p_3}$$

$$s_n = \frac{p_1 \cdot \cos x \cdot \cos y - s_d}{\cos^2 y + p_2 \cdot \sin^2 y}$$

where

$$x = \frac{ncol - COFF}{2^{-16} \cdot CFAC} \quad (\text{in Degrees})$$

$$y = \frac{nlin - LOFF}{2^{-16} \cdot LFAC} \quad (\text{in Degrees})$$

$$p_1 = 42164$$

$$p_2 = 1.006803$$

$$p_3 = 1737121856$$

$$CFAC = 13642337$$

$$LFAC = 13642337$$

The CFAC and LFAC coefficients are column and line scaling factors which depend on the specific segmentation approach of the input SEVIRI data. Finally, COFF and LOFF are coefficients depending on the location of the each Land-SAF geographical area within the Meteosat disk. These are included in the file metadata, and correspond to one set of the values detailed below per SEVIRI/MSG area:

Table A 5. Maximum values for number of columns (ncol) and lines (nlin), for each Land-SAF geographical area, and the respective COFF and LOFF coefficients needed to geo-locate the data.

Region Name	Description	Maximum ncol	Maximum nlin	COFF	LOFF
Euro	<u>E</u> urope	1701	651	308	1808
NAfr	<u>N</u> orthern <u>A</u> frica	2211	1151	618	1158
SAfr	<u>S</u> outhern <u>A</u> frica	1211	1191	-282	8
SAME	<u>S</u> outhern <u>A</u> merica	701	1511	1818	398
Disk	Full <u>D</u> isk	3712	3712	1857	1857